Available online at www.sciencedirect.com

SCIENCE DIRECT®

ELSEVIER

Journal of Contaminant Hydrology 74 (2004) 253–264

JOURNAL OF Contaminant Hydrology

www.elsevier.com/locate/jconhyd

Three-dimensional diffusion of non-sorbing species in porous sandstone: computer simulation based on X-ray microtomography using synchrotron radiation

Yoshito Nakashima[a,*], Tsukasa Nakano[a], Koichi Nakamura[a], Kentaro Uesugi[b], Akira Tsuchiyama[c], Susumu Ikeda[d]

[a] *National Institute of Advanced Industrial Science and Technology, Higashi 1-1-1 Central 7, Tsukuba, Ibaraki 305-8567, Japan*

[b] *Japan Synchrotron Radiation Research Institute (JASRI/SPring-8), Mikazuki, Hyogo 679-5198, Japan*

[c] *Department of Earth and Space Science, Graduate School of Science, Osaka University, Toyonaka, Osaka 560-0043, Japan*

[d] *Department of Complexity Science and Engineering, Graduate School of Frontier Sciences, The University of Tokyo, Kashiwanoha, 5-1-5, Kashiwa, Chiba 227-8651, Japan*

Received 8 March 2004; received in revised form 8 March 2004; accepted 25 March 2004

Abstract

The diffusion pathways of porous sandstone were examined by a three-dimensional (3-D) imaging technique based on X-ray computed tomography (CT) using the SPring-8 (Super Photon ring-8 GeV, Hyogo, Japan) synchrotron radiation facility. The analysis was undertaken to develop better understanding of the diffusion pathways in natural rock as a key factor in clarifying the detailed mechanism of the diffusion of radionuclides and water molecules through the pore spaces of natural barriers in underground nuclear waste disposal facilities. A cylindrical sample (diameter 4 mm, length 6 mm) of sandstone (porosity 0.14) was imaged to obtain a 3-D image set of 450^3 voxels = 2.62^3 mm^3. Through cluster-labeling analysis of the 3-D image set, it was revealed that 89% of the pore space forms a single large pore-cluster responsible for macroscopic diffusive transport, while only 11% of the pore space is made up of isolated pores that are not involved in long-range diffusive transport. Computer simulations of the 3-D diffusion of non-sorbing random walkers in the largest pore cluster were performed to calculate the surface-to-volume ratio of the pore, tortuosity (diffusion coefficient in free space divided by that in porous rock). The results showed that (i) the simulated surface-to-volume ratio is about 60% of the results obtained by conventional pulsed-field-gradient proton nuclear magnetic resonance (NMR) laboratory experiments and (ii) the simulated tortuosity is five to seven times larger than the results of laboratory diffusion experiments using non-

* Corresponding author. Fax: +81-29-861-3618.

E-mail address: nakashima.yoshito@aist.go.jp (Y. Nakashima).

0169-7722
doi:10.1016/j.jconhyd.2004.03.002

sorbing I^- and Br^-. These discrepancies are probably attributed to the intrinsic sample heterogeneity and limited spatial resolution of the CT system. The permeability was also estimated based on the NMR diffusometry theory using the results of the random walk simulations via the Kozeny–Carman equation. The estimated permeability involved an error of about 20% compared with the permeability measured by the conventional method, suggesting that the diffusometry-based NMR well logging with gradient coils is applicable to the in-situ permeability measurement of strata. The present study demonstrated that X-ray CT using synchrotron radiation is a powerful tool for obtaining 3-D pore structure images without the beam-hardening artifacts inevitable in conventional CT using X-ray tubes.

Keywords: Diffusion coefficients of iodine and bromine; NMR geophysical exploration; Pulsed-field-gradient stimulated-echo NMR; Pore structure NMR logging; Porous media

1. Introduction

In the underground disposal of nuclear waste, radionuclides (e.g., ^{129}I) migrate in water-saturated porous rocks by diffusion or random walk. Although there have been many studies on diffusion in rocks (e.g., Ohlsson and Neretnieks, 1995), there is little literature on the quantitative analysis of the three-dimensional (3-D) pore structure of natural porous rocks in terms of diffusion associated with nuclear waste disposal. The specific diffusion pathways (tortuous and irregular pores in natural rocks) need to be studied in order to understand the detailed mechanism of diffusion in these environments.

X-ray computed tomography (CT) is a powerful tool for obtaining the 3-D pore structure of porous media with high resolution (e.g., Wildenschild et al., 2002). The X-ray CT technique using synchrotron radiation was applied to the study of natural sandstone in the present study (Nakashima et al., 2003), and cluster-labeling image analysis (e.g., Ikeda et al., 2000) of the obtained CT images was performed to examine the pore connectivity (i.e., to count the pore voxels forming a large pore-cluster responsible for macroscopic diffusive transport).

Computer simulations of the diffusion of non-sorbing random walkers in the pore space have also been carried out to estimate the tortuosity (diffusion coefficient of non-sorbing ions in bulk water divided by that in the water-saturated porous rock) and surface-to-volume ratio of the pores. The estimated quantities have been compared with measurements by conventional laboratory experiments (i.e., diffusion experiments on non-sorbing I^-, Br^-, and H_2O). Previous synchrotron CT studies on porous rocks (e.g., Spanne et al., 1994; Ferreol and Rothman, 1995) have tended to focus on the Darcy flow simulations, and there is no detailed research targeting diffusion. To the best of the authors' knowledge, the present study is the first application of synchrotron microtomography to the study of diffusive migration of non-sorbing species in porous rocks.

Nakashima and Watanabe (2002) proposed a new method for the in-situ measurement of the permeability of strata, which is applicable to the formation characterization of the nuclear waste disposal sites. The method was derived from the nuclear magnetic resonance (NMR) diffusometry theory, and its advantage over the conventional NMR well logging

based on the T2-relaxometry (e.g., Dunn et al., 2002) is that permeabilities can be estimated without the information of the rock species. However, the applicability of the diffusometry-based method to natural rocks has not been tested. Thus, we estimated the sandstone permeability using the diffusion data (tortuosity and surface-to-volume ratio) obtained by the computer simulations to compare with the permeability measured by the conventional laboratory experiments.

2. Experimental

The "SP-μCT" X-ray CT system of the SPring-8 synchrotron radiation facility (Super Photon ring 8 GeV, Hyogo, Japan) was employed for tomography in the present study. SP-μCT was developed at the BL20B2 beam line for imaging rocks and minerals at an effective spatial resolution of about 13 μm (Uesugi et al., 1999; Ikeda et al., 2004). Although X-ray CT is capable of obtaining the 3-D internal structure of rocks, some artifacts occur. "Beam-hardening", one of the most serious artifacts, originates from the polychromatic energy distribution of the X-ray source used (e.g., Ketcham and Carlson, 2001; Nakashima, 2003). The advantage of SP-μCT over conventional microfocus CT using X-ray tubes is that the synchrotron radiation provides monochromatic X-rays, effectively eliminating beam-hardening.

The imaging conditions were as follows. The monochromatic X-ray energy was 25 keV. A total of 360 projections were made through 180° sample-rotation, with an X-ray exposure time of 12 s per projection. The time required for acquisition of the 360 projections was about 80 min. The convolution back-projection method using a Chesler filter was used to reconstruct an 8-bit 3-D CT image set (710 contiguous two-dimensional slices, 1000 × 1000 voxels each slice). The voxel (volume element) of the CT image was cubic, with side lengths of 5.83^3 μm^3.

A cylindrical sample (diameter 4 mm, length 6 mm) of sandstone collected from a Tertiary formation in Chichibu, Japan was prepared for the SP-μCT experiment. The grain size of the sandstone was about 0.1 mm, with major mineral constituents of quartz and plagioclase and minor strong X-ray absorbers (biotite, goethite, and zircon). The bulk density of the dry sandstone sample was 2.2 g/cm^3, and the porosity measured by the difference between water-saturated and dry sample weights of a known volume was 0.14. Permeabilities of five cylindrical sandstone blocks (diameter 30 mm, length 50 mm) were measured by a conventional permeability test to obtain 1.3×10^{-14} m^2.

The surface-to-volume ratio of the pore space and tortuosity is important transport properties of porous media. These properties were estimated in the present study directly by computer simulations of diffusion using the obtained CT images. The two quantities were measured also by the following laboratory experiments for comparison. The pulsed-field-gradient stimulated-echo proton NMR technique allows the surface-to-volume ratio to be measured by measuring the time-dependent self-diffusion coefficient of pore water molecules (e.g., Balzarini et al., 1996). This NMR technique was applied to a water-saturated sample (diameter 7.5 mm, length 30 mm) on an NMR spectrometer at 0.47 T and 23.6 °C, and the obtained surface-to-volume ratio of the pores was 3.9×10^5 m^{-1}. Because the proton transverse surface-relaxivity of the water-saturated sample was as

small as 5.6×10^{-5} m/s, a theoretical model for negligible surface-relaxivity (e.g., Eq. (B.4) of Dunn et al., 2002) was used in the calculation of the surface-to-volume ratio.

The tortuosity was measured by imaging the diffusion of heavy ions (I^- and Br^-) in water-saturated sandstone blocks ($4 \times 4 \times 2$ cm^3) using a medical X-ray CT scanner. KI and KBr were chosen as I- and Br-bearing substances. The principle of the diffusion experiments using X-ray CT is described at length by Nakashima (2000, 2003). According to the experiments, the tortuosity was estimated to be 4.7 by I^- diffusion and 3.4 by Br^- diffusion. The computer simulation in the present study was performed for the diffusion of non-sorbing random walkers so as to probe the geometrical tortuosity. Thus, the diffusants used in the laboratory experiments should also be non-sorbing. Therefore, H_2O, I^-, and Br^- were chosen as diffusants in the NMR and medical X-ray CT experiments.

3. Image analysis and random walk simulation

A cubic region of 450^3 voxels ($=2.62^3$ mm^3) was extracted from the original SP-μCT image set consisting of $1000 \times 1000 \times 710$ voxels. All image-analyses and random walk simulations were performed on this 450^3-voxel set. The 8-bit images (e.g., Fig. 1a) were graded such that voxel intensity of air-filled pores was low (low density), and that of the solid was high (high density). The intensity threshold for discriminating between solid and pores was chosen so as to yield the experimentally measured porosity (0.14). This porosity is the *effective porosity*, corresponding to the pore space forming a large percolation cluster connected to the sample surface, by which water infiltration is possible. Thus, the threshold was chosen such that the volume fraction of the largest pore cluster equaled the effective porosity of 0.14.

Cluster labeling (e.g., Stauffer and Aharony, 1994) is an image analysis technique for determining the connectivity of pore voxels. The volume and surface area are calculated for each cluster. This analysis was applied to the 3-D binary images of 450^3 voxels. The cluster neighborhood rule was based on Ikeda et al. (2000). The threshold for discriminating pores from the solid was determined by trial and error such that the volume fraction of the largest pore cluster was 0.14. The main purpose of cluster labeling is to extract the largest pore cluster responsible for macroscopic material transport across the image system. Random walk simulations were then performed on this largest pore cluster, and the contribution of isolated pores to the total porosity was also estimated.

3-D random walk computer simulations on the largest pore cluster were performed to calculate the tortuosity. Two Mathematica® programs, RW3D.m (Watanabe and Nakashima, 2002) and DMAP.m (Nakashima and Yamaguchi, 2004a,b), available for free download from the author's homepage (URL http://staff.aist.go.jp/nakashima.yoshito/progeng.htm) were used for the simulations. The random walk algorithm used in the programs was a lattice walk in a simple cubic lattice (e.g., Stauffer and Aharony, 1994), and non-sorbing walkers migrate on the discrete voxels whose gray-levels correspond to pore space. The random walkers should be non-sorbing because the purpose is to calculate the geometrical tortuosity and the undesirable effects of the sorption of walkers on the solid surface should be eliminated. In the algorithm, a voxel is chosen randomly as a start position of the lattice walk trial at $t_{int} = 0$ where t_{int} is the dimensionless integer time. The

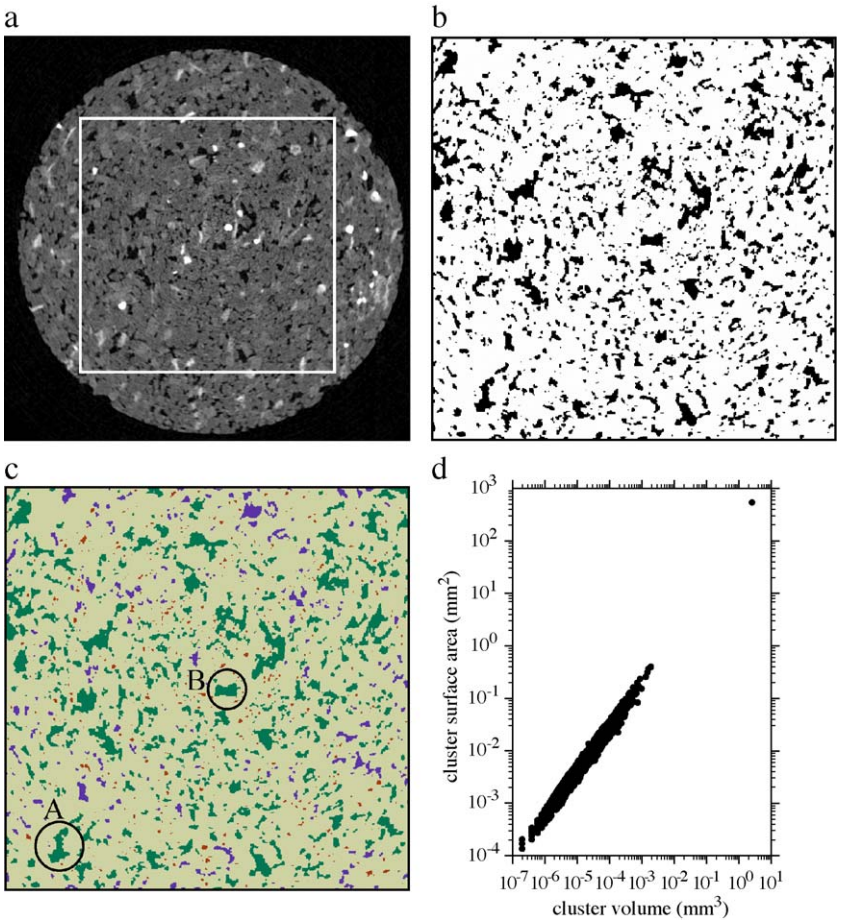

Fig. 1. Cluster labeling of pores in the sandstone. (a) Example of an 8-bit 2-D CT image of a cylindrical dry sandstone sample (diameter 4 mm). The image dimension is 725^2 voxels = 4.23^2 mm^2. The square region (open frame) of 450^2 voxels was extracted for 3-D cluster labeling analysis. (b) Binary (i.e., 1-bit) image of the square region in (a), obtained assuming a threshold value yielding an effective porosity of 0.14. Black voxels represent pores, and white voxels represent the solid. (c) Result of cluster labeling for region (b). Coloring scheme is as noted in Table 1. Note that the green clusters in circles A and B are connected three-dimensionally. (d) Cross-plot of the volume and surface area of each pore cluster. A total of 122,207 pore clusters were identified (Table 1). The volume and surface area of the largest pore cluster (green in Fig. 1c) are 12,843,767 voxels = 2.55 mm^3 and 5.40×10^2 mm^2, respectively.

walker executes a random jump to one of the nearest unoccupied sites; t_{int} is incremented by unit time after the jump so that the time becomes $t_{int} + 1$. If the randomly selected site or voxel is occupied by an obstacle or solid, the jump is not performed, but the time becomes $t_{int} + 1$. RW3D.m gave the time-dependent mean-square displacement of the non-sorbing walkers, from which the diffusion coefficient could be calculated by taking the time-derivative. RW3D.m also allows the surface-to-volume ratio of the pore space to be

estimated by measuring the time-dependent diffusion coefficient (Nakashima and Watanabe, 2002). DMAP.m simulates the "out-diffusion" laboratory experiments (e.g., Sardini et al., 2003), and the lattice walk is carried out until the walker goes out of the 450^3 image system. The time required for each walker to escape from the 450^3 system is recorded to calculate the cumulated flux (i.e., integrated number of walkers escaped from the system by the time t_{int}). The tortuosity can be estimated by fitting the time-dependent cumulated flux to a theoretical curve (Nakashima and Yamaguchi, 2004a,b). The simulated values of tortuosity and surface-to-volume ratio were then compared with the results obtained by laboratory diffusion experiments on non-sorbing H_2O, I^-, and Br^-.

It is possible to predict the permeability of porous media using the diffusion data via empirical Kozeny–Carman equation (Nakashima and Watanabe, 2002). Assuming an orthogonal network of cylindrical tortuous pipes of equiradii and the Poiseuille flow in the pipes (Nakashima and Yamaguchi, 2004a), we obtained 1/6 for the correction factor, α, of Eq. (5) of Nakashima and Watanabe (2002):

$$k = \frac{\phi}{6\left(\frac{D_0}{D_\infty}\right)\left(\frac{S}{V}\right)^2_{\text{pore}}} \tag{1}$$

where k is the permeability, ϕ is the porosity, D_∞ is the diffusion coefficient of the non-sorbing random walkers in the porous media in the limit of $t_{int} \rightarrow \infty$, D_0 is that in the free space (i.e., $\phi = 1$), and $(S/V)_{pore}$ is the surface-to-volume ratio of the pore space. The ratio, D_0/D_∞, is the tortuosity of the pore structure. Results of the random walk simulations on the largest pore cluster by RW3D.m and DMAP.m were substituted into Eq. (1) to predict the sandstone permeability.

4. Results and discussion

An example of the 8-bit SP-μCT images is shown in Fig. 1a. The voxel intensity (CT number) increases with increasing density and atomic number of the minerals. Quartz and plagioclase are dark, air-filled pores are the darkest, and Fe- and Zr-bearing strong X-ray absorbers (biotite, goethite, and zircon) are bright in the image. Beam-hardening (e.g., Nakashima, 2003) is negligible in Fig. 1a, ensuring accurate cluster-labeling analysis. The air-filled voxels in the square region of Fig. 1a are extracted to obtain a binary image (Fig. 1b). A total of 450 contiguous 2-D binary images were analyzed by cluster labeling.

The results of the cluster-labeling analysis are shown in Figs. 1c–d and 2, and listed in Table 1. An important aspect of this 3-D image analysis is demonstrated in Fig. 1c. Although the two green regions in circles A and B do not appear to be connected on the 2-D slice, the regions are in fact connected three-dimensionally to form a single large pore cluster. This suggests that conventional 2-D studies of the pore connectivity by microscopy analysis of a single thin-section are probably misleading. The largest cluster (green in Fig. 2a,b) depicts the complex tortuous 3-D network of pores, which is difficult to obtain by other imaging methods such as 2-D optical microscopy. A total of 122,207 pore clusters were identified, and a single large percolation-cluster was recognized, responsible for

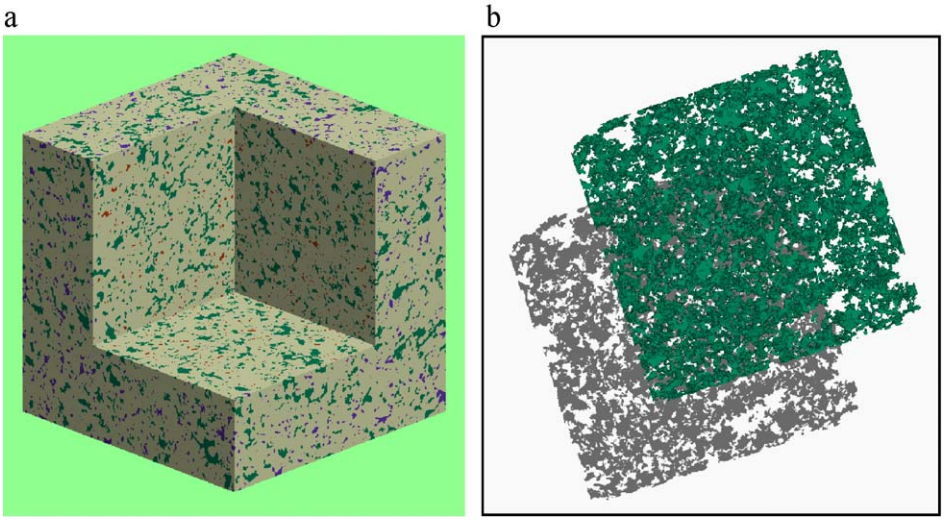

Fig. 2. Pore structure of the sandstone sample. (a) 3-D image of pore clusters. The image dimension is 450^3 voxels = 2.62^3 mm^3. Colors are the same as noted in Table 1. (b) Shaded part (slab of $450 \times 450 \times 40$ voxels = $2.62 \times 2.62 \times 0.233$ mm^3) extracted from (a). Only the largest pore cluster (green) is visualized.

macroscopic material transport by diffusion (Fig. 1d). Fig. 1d shows that the volume fraction and surface-to-volume ratio of the largest pore cluster are 12,843,767/$450^3 \approx 0.141$ and 5.40×10^2 mm^2/2.55 $mm^3 \approx 2.1 \times 10^5$ m^{-1}, respectively.

Cluster labeling (Fig. 1d) revealed that, except for the largest cluster, there are 122,206 pore clusters, which are probably isolated from the cylindrical sample surface and thus never contribute to long-range diffusive transport. It is possible to estimate the volume fraction of such isolated pores (purple and brown voxels in Figs. 1c and 2a). The total voxel-numbers of the isolated pores and of the largest pore cluster are 1,650,114 and 12,843,767, respectively. Thus, 12,843,767/(12,843,767 + 1,650,114) = 89% of the pore space forms a single large pore-cluster responsible for macroscopic diffusive transport, while 1,650,114/(12,843,767 + 1,650,114) = 11% of the pore space represents isolated pores through which material transport across the 450^3 system is impossible. The volume fraction of the isolated pores is 1,650,114/450^3 = 0.018. Given the effective porosity (porosity of the largest pore

Table 1
Results of cluster labeling analysis of pore voxels in the 450^3 system

Color of voxels	Volume fraction	Number of pore clusters	Total surface area (mm^2)
Green	0.141	1	540
Purple	0.004	4218	21
Brown	0.014	117,988	117
Pale yellow	0.841	–	–
Total	1	122,207	678

Green: largest pore cluster. Purple: pore clusters, except for the green cluster, connected to at least one of the six square surfaces of the cubic 450^3 system. Brown: pore clusters isolated from the six surfaces of the cube. Pale yellow: solid grains.

cluster) of 0.141, the total porosity of the 450^3 system is $0.141 + 0.018 = 0.159$ (Table 1). This is very close to the total porosity of $1 - 2.2/2.65 \approx 0.17$ determined experimentally based on the measured bulk density of the dry sample (2.2 g/cm^3) and assuming an average grain density of 2.65 g/cm^3 (i.e., grain density of quartz). Thus, it is considered that cluster-labeling analysis was performed in a reliable manner.

All pore clusters except for the largest cluster are classified into two groups: clusters connected to at least one of the six surfaces of the 450^3 cube (purple); or clusters isolated from the six surfaces (brown) (Fig. 2a and Table 1). Some of the purple clusters may connect to the largest pore cluster if the system size for the cluster labeling is larger than 450^3 voxels. Although such purple clusters should be considered in the calculation of the effective porosity and in the determination of the threshold value, the connection of these clusters was neglected in the present study because the fraction of such clusters cannot be determined. Fortunately according to the cluster-labeling results, the porosity of the all purple clusters is 0.004 (Table 1), which is much smaller than the porosity of the largest cluster (0.141) and can be reasonably neglected.

The results of the lattice walk using RW3D.m are shown in Fig. 3. The non-sorbing walkers migrate via the largest pore cluster (green voxels in Fig. 2a), avoiding obstacles (brown, purple, and pale yellow voxels). The mean-square displacement shows that diffusion through the pores is strongly restricted by the tortuous pore structure (Fig. 3b). The tortuosity is the ratio of the slope of the mean-square displacement in the free space to that in the sandstone pore in the limit of $t_{\mathrm{int}} \rightarrow \infty$, and was calculated to be 23 in Fig. 3b. The surface-to-volume ratio of the largest pore cluster can be estimated from diffusion data over a short time range. Because negligible surface-relaxivity is assumed in RW3D.m, the theoretical curve, Eq. (10) of Nakashima and Watanabe (2002), was fitted to the time-derivative of the mean-square displacement, giving a surface-to-volume ratio of 2.5×10^5 m^{-1} (Fig. 3c). This value agrees well with the value, 2.1×10^5 m^{-1}, determined by the cluster labeling analysis (Fig. 1d), suggesting that the random walk simulation was performed in a reliable manner.

The results of the random walk simulation using DMAP.m are shown in Fig. 4. This figure shows that the out-diffusion from the rock pores is delayed greatly owing to the tortuous pore structure compared to free space. The tortuosity value, 23, estimated by DMAP.m is equal to that by RW3D.m (Fig. 3b), demonstrating the reliability of the programs.

The transport properties obtained by cluster labeling and lattice walk simulations using SP-μCT data are compared with the results of conventional laboratory experiments in Table 2. Although the scatter of values falls within an order of magnitude, the discrepancy is not negligible. The surface-to-volume ratio of the pores was 50–60% of the result of the NMR experiment, and the simulated tortuosity was five to seven times larger than the results of laboratory diffusion experiments using I^- and Br^-. A similar discrepancy of a factors 3–5 was also reported for the prediction of sandstone permeability by Lattice–Boltzmann simulation using 3-D pore images of a small volume (O'Connor and Fredrich, 1999). This can be attributed to the intrinsic meso-scale heterogeneity of tortuosity in natural porous rocks (e.g., Gibbs et al., 1993), which would have been averaged in the larger samples used for laboratory NMR and medical X-ray CT experiments. The small sample (Fig. 2a) used for the computer simulations is several orders of magnitude less

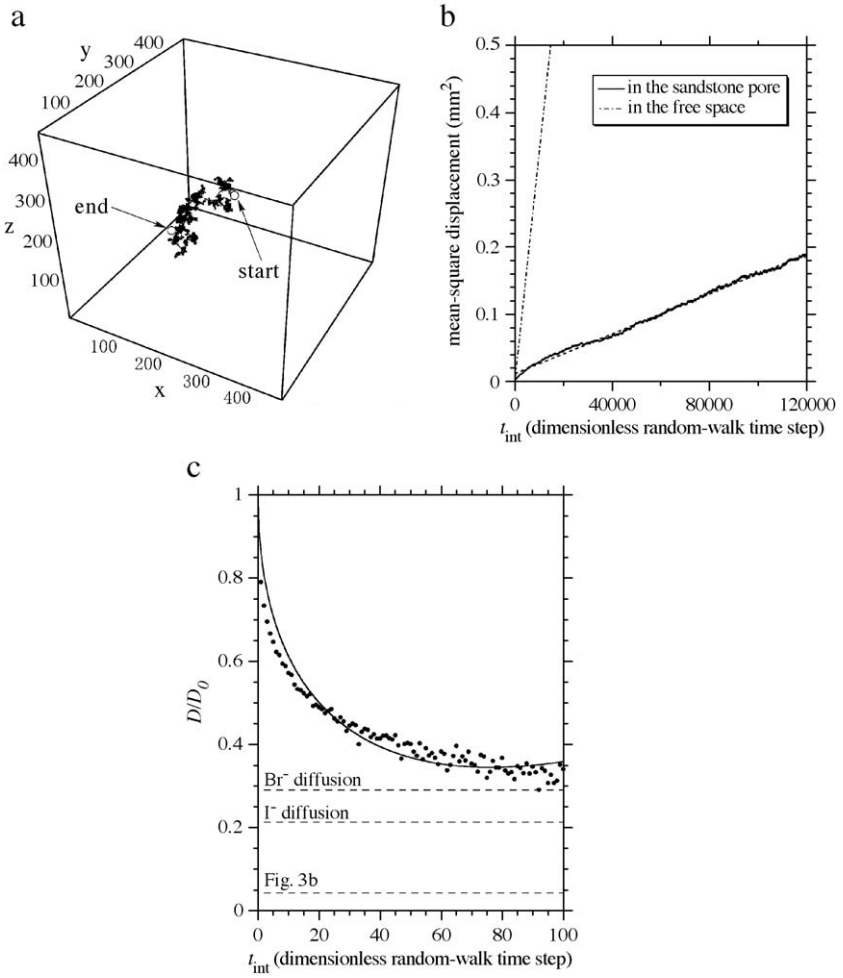

Fig. 3. Computer simulation of diffusion through the largest pore cluster (green voxels in Fig. 2a) using RW3D.m. (a) Example of 3-D trajectory of lattice walk for a single walker over 120,000 time steps. The initial and final positions are marked by open circles. (b) Mean-square displacement averaged over 400 walkers as a function of dimensionless integer time, t_{int}. The linear regression analysis (dotted line) was applied to the data points for large t_{int} (i.e., t_{int}>20,000) to obtain the tortuosity of 23. The simulation was completed in 303 h using a personal computer with a 1.5-GHz Pentium® 4 processor. The theoretical mean-square displacement, Eq. (8) of Nakashima and Watanabe (2002), for the lattice walk in the free space (i.e., $\phi = 1$) is also indicated. (c) Short-time behavior of the normalized diffusivity of walkers averaged over 150,000 walkers. The time-derivative of the mean-square displacement was calculated using the backward difference scheme, and translated into the normalized diffusivity, D/D_0, where D is the time-dependent diffusivity of the non-sorbing walkers in the porous rock. The simulation was completed in 2.5 h using the same personal computer as (b). A theoretical curve, Eq. (10) of Nakashima and Watanabe (2002), was fitted to the D/D_0 data to obtain the surface-to-volume ratio to be 2.5×10^5 m^{-1}. In the limit of $t_{int} \rightarrow \infty$, the D/D_0 value reaches the reciprocal number of the tortuosity listed in Table 2, and is indicated as asymptote (broken line) for the I^- and Br^- diffusion tests and computer simulation of Fig. 3b.

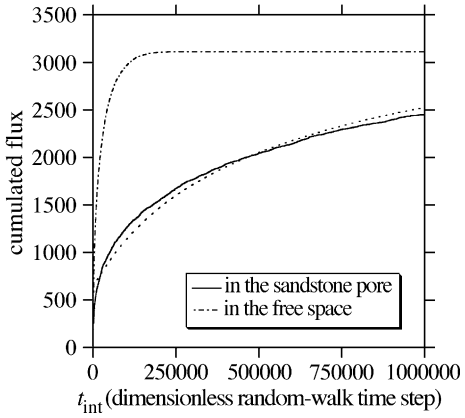

Fig. 4. Computer simulation of out-diffusion for the largest pore cluster using DMAP.m. The cumulated flux (integrated number of walkers escaping from the 450^3 system) is shown as a function of the dimensionless integer time, t_{int}. The theoretical model (dotted curve), Eq. (10) of Nakashima and Yamaguchi (2004a), was fitted to the data to obtain the tortuosity of 23. The number of random walkers is 3114. The simulation was completed in 174 h using the same personal computer as Fig. 3b. The theoretical curve for the random walk in the free space (i.e., $\phi = 1$) is also shown for the same number of the walkers.

voluminous than the samples used in the laboratory experiments, and would be highly susceptible to localized variations in these values.

Another possible explanation for the discrepancy is the finite spatial resolution of the CT system. The average pore diameter of porous media can be estimated to be $4/(S/V)_{pore}$ if cylindrical pipes of equiradii are assumed for the pore structure (Guéguen and Palciauskas, 1994). It is $6/(S/V)_{pore}$ if spherical pores of equiradii are assumed. According to the pulsed-field-gradient stimulated-echo NMR, $(S/V)_{pore}$ is 3.9×10^5 m^{-1} (Table 2) giving $4/(S/V)_{pore} = 10$ μm and $6/(S/V)_{pore} = 15$ μm. These values are on the same order as the voxel dimension (5.83 μm) and effective spatial resolution (13 μm) of the CT system. The estimated average pore-diameter suggests that some fractions of the pores in the sandstone are less than the voxel dimension or spatial resolution because the pore size distribution of sedimentary rocks ranges within several orders of magnitude (e.g., Dunn et

Table 2
Comparison of transport properties of the Chichibu sandstone obtained by image analysis and computer simulation using SP-μCT data and by conventional laboratory experiments

Quantity	SP-μCT study	Laboratory experiments
Effective porosity[a]	0.141 (Table 1)	0.14
Total porosity	0.159 (Table 1)	0.17
Surface-to-volume ratio	2.1×10^5 m^{-1} (Fig. 1d)	3.9×10^5 m^{-1}
	2.5×10^5 m^{-1} (Fig. 3c)	
Tortuosity	23 (Fig. 3b)	4.7 (I^- diffusion)
	23 (Fig. 4)	3.4 (Br^- diffusion)
Permeability	1.6×10^{-14} m^2 (Eq. (1))	1.3×10^{-14} m^2

[a] The effective porosity determined by the SP-μCT study was derived so as to be equal to the experimental result.

al., 2002). According to Keller (1998), pores and fractures as small as 13% of the voxel size can be detected by the partial-volume effect. On the other hand, for example, it is probably difficult to image pores of several tens of nanometers in diameter by the CT system used. Thus, some fractions of the submicron-scale pores in the sandstone were probably ignored, and the contribution of the small channels to the diffusive transport and $(S/V)_{pore}$ was neglected. This is a possible cause for the overestimate of the tortuosity and underestimate of $(S/V)_{pore}$ in Table 2.

The permeability was estimated by the diffusometry. The results of the random walk simulations (i.e., $D_0/D_\infty = 23$ and $(S/V)_{pore} = 2.5 \times 10^5\ m^{-1}$), and $\phi = 0.14$ were substituted into Eq. (1) to obtain $k = 1.6 \times 10^{-14}\ m^2$ (Table 2). If the values by laboratory experiments (i.e., $D_0/D_\infty = 3.4$ and $(S/V)_{pore} = 3.9 \times 10^5\ m^{-1}$) are used, k is $4.5 \times 10^{-14}\ m^2$. These predicted k-values fall within an order of magnitude when compared with the experimentally measured value ($1.3 \times 10^{-14}\ m^2$). The estimation error (less than an order of magnitude) is equal to or better than that in the conventional NMR logging based on the T2-relaxometry (Straley et al., 1997). Thus, although more tests are required, the present study suggests that the lithology-independent method using Eq. (1) is useful in the in-situ measurement of permeabilities of strata by NMR well logging.

The present study demonstrated that X-ray CT is useful for obtaining high-resolution 3-D pore images non-destructively and quickly. The use of synchrotron radiation allows us to (i) obtain CT images of pore structure without beam-hardening artifacts at voxel dimensions of several microns (this study) or even at the submicron level (Uesugi et al., 2001) and (ii) map the 3-D distribution of Cs concentration using an absorption edge (Ikeda et al., 2004). Thus, X-ray CT using synchrotron radiation is expected to be a powerful tool in the study of diffusion relevant to nuclear waste disposal.

Acknowledgements

Comments by the anonymous reviewers were helpful. SP-μCT experiments were performed at the SPring-8 facility with the approval of the Japan Synchrotron Radiation Research Institute (Proposal No. 2001B0501-NOD-np). This study was supported by the Budget for Nuclear Research of the Ministry from Education, Culture, Sports, Science and Technology, of Japan based on screening and counseling by the Atomic Energy Commission.

References

Balzarini, M., Pavesi, L., Deriu, A., 1996. Resiricted geometry fluid dynamics in natural porous systems by QENS and NMR PGSE. Phys., B Condens. Matter 226, 10–14.

Dunn, K.-J., Bergman, D.J., Latorraca, G.A., 2002. Nuclear Magnetic Resonance Petrophysical and Logging Applications. Pergamon, Amsterdam. 293 pp.

Ferreol, B., Rothman, D.H., 1995. Lattice–Boltzmann simulations of flow-through Fontainebleau sandstone. Transp. Porous Media 20, 3–20.

Gibbs, S.J., Attard, J.J., Hall, L.D., 1993. Diffusion in brine-saturated reservoir cores studied by NMR imaging. AIChE J. 39, 689–694.

Guéguen, Y., Palciauskas, V., 1994. Introduction to the Physics of Rocks. Princeton Univ. Press, Princeton. 294 pp.

Ikeda, S., Nakano, T., Nakashima, Y., 2000. Three-dimensional study on the interconnection and shape of crystals in a graphic granite by X-ray CT and image analysis. Min. Mag. 64, 945–959.

Ikeda, S., Nakano, T., Tsuchiyama, A., Uesugi, K., Suzuki, Y., Nakamura, K., Nakashima, Y., Yoshida, H., 2004. Nondestructive three-dimensional element-concentration mapping of a Cs-doped partially molten granite by X-ray computerized tomography using synchrotron radiation. Am. Mineral. (in press).

Keller, A., 1998. High resolution, non-destructive measurement and characterization of fracture apertures. Int. J. Rock Mech. Min. Sci. 35, 1037–1050.

Ketcham, R.A., Carlson, W.D., 2001. Acquisition, optimization and interpretation of X-ray computed tomographic imagery: applications to the geosciences. Comput. Geosci. 27, 381–400.

Nakashima, Y., 2000. The use of X-ray CT to measure diffusion coefficients of heavy ions in water-saturated porous media. Eng. Geol. 56, 11–17.

Nakashima, Y., 2003. Diffusivity measurement of heavy ions in Wyoming montmorillonite gels by X-ray computed tomography. J. Contam. Hydrol. 61, 147–156.

Nakashima, Y., Watanabe, Y., 2002. Estimate of transport properties of porous media by micro-focus X-ray computed tomography and random walk simulation. Water Resour. Res. 38 (paper number 1272, DOI number 10.1029/2001WR000937).

Nakashima, Y., Yamaguchi, T., 2004a. Original free Mathematica® programs for the calculation of transport properties of porous media. In: Otani, J., Obara, Y. (Eds.), X-ray CT for Geomaterials; Soils, Concrete, Rocks. A.A. Balkema, Lisse, Netherlands, pp. 103–110.

Nakashima, Y., Yamaguchi, T., 2004b. DMAP.m: a Mathematica® program for the three-dimensional mapping of the diffusivity and porosity of heterogeneous porous media. Bull. Geol. Surv. Japan (in review).

Nakashima, Y., Nakano, T., Nakamura, K., Uesugi, K., Tsuchiyama, A., Ikeda, S., 2003. 3-D imaging of diffusion paths in porous sandstones by X-ray microtomography using synchrotron radiation. Abstracts of the MIGRATION'03 Conference (9th International Conference on Chemistry and Migration Behavior of Actinides and Fission Products in the Geosphere), Gyeongju, Korea, September 21–26, 132.

O'Connor, R.M., Fredrich, J.T., 1999. Microscale flow modelling in geologic materials. Phys. Chem. Earth 24, 611–616.

Ohlsson, Y., Neretnieks, I., 1995. Literature survey of matrix diffusion theory and of experiments and data including natural analogues. SKB Technical Report (Swedish Nuclear Fuel and Waste Management) TR95-12, 1–88.

Sardini, P., Delay, F., Hellmuth, K.-H., Porel, G., Oila, E., 2003. Interpretation of out-diffusion experiments on crystalline rocks using random walk modeling. J. Contam. Hydrol. 61, 339–350.

Spanne, P., Thovert, J.F., Jacquin, C.J., Lindquist, W.B., Jones, K.W., Adler, P.M., 1994. Synchrotron computed microtomography of porous media: topology and transports. Phys. Rev. Lett. 73, 2001–2004.

Stauffer, D., Aharony, A., 1994. Introduction to Percolation Theory, Revised 2nd edition Taylor & Francis, London. 192 pp.

Straley, C., Rossini, D., Vinegar, H., Tutunjian, P., Morriss, C., 1997. Core analysis by low-field NMR. Log Anal. 38 (2), 84–94.

Uesugi, K., Tsuchiyama, A., Nakano, T., Suzuki, Y., Yagi, N., Umetani, K., Kohmura, Y., 1999. Development of micro-tomography imaging system for rock and mineral samples. Presented at the SPIE Conference on Developments in X-Ray Tomography II, Denver, Colorado, July, 1999. Proceedings of SPIE, vol. 3772, pp. 214–221.

Uesugi, K., Suzuki, Y., Yagi, N., Tsuchiyama, A., Nakano, T., 2001. Development of high spatial resolution X-ray CT system at BL47XU in SPring-8. Nucl. Instrum. Methods Phys. Res., Sect. A, Accel. Spectrom. Detect. Assoc. Equip. 467, 853–856.

Watanabe, Y., Nakashima, Y., 2002. RW3D.m: three-dimensional random walk program for the calculation of the diffusivities in porous media. Comput. Geosci. 28, 583–586.

Wildenschild, D., Hopmans, J.W., Vaz, C.M.P., Rivers, M.L., Rikard, D., Christensen, B.S.B., 2002. Using X-ray computed tomography in hydrology: systems, resolutions, and limitations. J. Hydrol. 267, 285–297.